Electronic Supplementary Material (ESI) for Physical Chemistry Chemical Physics.

Influence of argon and D_2 tagging on the hydrogen bond network in $Cs^+(H_2O)_3$; Kinetic trapping below 40 K.

Tim K. Esser,[a] Harald Knorke,[a] Flavio Siro-Brigiano,[b] Daria Ruth Galimberti,[b] Knut R. Asmis,[a*] Marie-Pierre Gaigeot,[b*] James M. Lisy[d*]

[a] *Wilhelm-Ostwald-Institut für Physikalische und Theoretische Chemie, Universität Leipzig, Linnéstrasse 2, D-04103 Leipzig, Germany.*

[b] *LAMBE UMR8587, Univ Evry, Université d'Evry Val d'Essonne, CNRS, CEA, Université Paris-Saclay, 91025 Evry, France*

[d] *Department of Chemistry, University of Illinois at Urbana–Champaign, Urbana, Illinois 61801, United States*

* E-mail: knut.asmis@uni-leipzig.de, mgaigeot@univ-evry.fr, j-lisy@illinois.edu

Supporting Information

Computational details

Untagged and Ar-/D_2-tagged structures of $Cs^+(H_2O)_3$ clusters have been optimized at the MP2 and DFT-B3LYP-D3 levels of electronic representation, with the Gaussian09 package.[1] The MP2 electronic representation serves as reference for the B3LYP corrected for dispersion effects (Grimme D3 correction[2] in the Becke and Johnson damping scheme GD3BJ[3]). All calculations are performed with the Los Alamos double-zeta basis set[4] with an effective core potential for Cs, and the correlated all-electron basis set aug-cc-PVDZ[5] for all other atoms. Harmonic frequencies have been systematically calculated in order to check for minima on the potential energy surface, and are further used for harmonic vibrational spectra in order to interpret and assign the experimental IRPD spectra. To that end, harmonic frequencies are scaled by a 0.9686 factor[6], very close to the 0.97 scaling factor used in previous work by the Lisy group[7] and found by the systematic alignment of the O-H stretching band position between calculation and experiment for the $Cs^+(H_2O)_2$ cluster.[8]

Optimized geometries are reported in Figure 2 in the main text, for untagged and Ar/D_2 tagged $Cs^+(H_2O)_3$ clusters. Four conformers are identified for the untagged $Cs^+(H_2O)_3$ cluster, labeled by I-IV Roman numeral (by increasing order of energy). The associated tagged $Cs^+(H_2O)_3$ conformers are reported with a Roman numeral-number coding, e.g. I-2, III-1, etc. The number does not necessarily refer to the energy order. We have instead organized the tagged conformers into two groups: the first group with numbers ranging from 1 to 3 correspond to Ar/D_2-$Cs^+(H_2O)_3$ conformers where the tag is weakly interacting with water molecule(s), while the tag is interacting with the Cs^+ cation in the second group labeled with numbers 4-6. The reference of energy is the untagged I-conformer for untagged clusters, while it is the I-1 conformer for tagged-clusters. For the four untagged clusters, we have reported rankings in electronic energies, the Vibrational Zero Point Energy ZPE, and in free energies calculated at 20 K (E, E^{ZPE}, and ΔG_{20K}, respectively in fig 2).

To estimate the role in entropy into the relative stability of the conformers at finite temperatures, free energy profiles have also been calculated for the untagged I-IV interconversion and for the stability of the III cluster, at different temperatures. This is done through biased metadynamics DFT-BLYP-D3 based molecular dynamics simulations using the CP2K code.[9] The mixed Gaussian DZVP-Molopt-Short Range basis set and 400 Ry energy cut-off plane wave basis set are used in the DFT-MD metadynamics, together with GTH pseudo-potentials.[10] The clusters are simulated in a box of 25x25x25 Å^3 dimensions, the Poisson equations are solved through the Martyna-Tuckerman method for non-periodic systems.[11] The BLYP-D3 DFT-MD representation has been tested against the B3LYP-D3 all electron representation, giving the same optimized I-IV geometries and same energy ranking.

Metadynamics are performed with a time step of 0.4 fs in the NVT canonical ensemble, at the three temperatures of 10 K, 20 K, and 50 K. 50 initial configurations have been chosen, each one of them starts from the I-untagged $Cs^+(H_2O)_3$ cluster for the I-IV conversion. The same procedure has been followed starting from the III-untagged $Cs^+(H_2O)_3$ cluster to predict the free energy evolution with temperature for this cluster.

Each starting configuration (positions and velocities) is randomly chosen from an equilibrated trajectory, such that the starting Metadynamics points sample a Boltzmann distribution. Metadynamics are performed using the CSVR thermostat with a short time constant of 16 fs. With the low number of degrees of freedom for the $Cs^+(H_2O_3)$ cluster, a rescaling of the velocities was also applied whenever the instantaneous temperature was found out of the target temperature by +/-10K. The bias is chosen along the OW-OW distance between one of the two H-bonded water molecules of conformer I (or III). The biased Metadynamics are run with hills of 10^{-3} Hartree height and 0.05 Å width, with the addition of a new hill every 100 time-steps. Runs are done until free energy wells have been filled.

Four lower-energy conformers of the untagged $Cs^+(H_2O)_3$ cluster have been optimized within an energy spread of ≈13.0(MP2)/8.0(B3LYP-D3) kJ/mol when the electronic energies are corrected for ZPE vibrational zero point energy contributions (without ZPE corrections, the spread increases to 26.0/18.0 kJ/mol respectively for MP2 and B3LYP-D3). See Table 1 and Figure 2 in the main text. Three structures are identical to those reported earlier,[7, 8, 12] while the slight difference in the IV-structure will be discussed below. The B3LYP-D3 relative energies reproduce the MP2 ones remarkably well (ZPE and no-ZPE corrections), providing the same energy ranking as the MP2 level. The energy difference between the III-IV higher energy conformers is however reduced at the B3LYP-D3 level compared to MP2. See Table 1 in the main text.

The geometrical details given below for the four optimized structures are based on the B3LYP-D3 calculations. I and II are the two lower energy conformers. They are quasi-isoenergetic (energies within 2.0 kJ/mol) and their energy ranking depends on the inclusion of ZPE contributions. MP2 and B3LYP-D3 results are identical (within the ab initio uncertainties). Although quasi-isoenergetic, the structures of these two conformers differ considerably. In the I conformer, Cs^+ symmetrically interacts with two water molecules (Cs^+-OW distances are 3.1 Å), while the third water is located in the second solvation shell and accepting two H-Bonds from the first shell water molecules. In the II conformer, the three water molecules are forming a H-bonded water trimer while the cation is located symmetrically above the water trimer, out of the plane formed by the O-H bonded groups, simultaneously interacting with all three water molecules from somewhat longer distances (the 3 Cs^+-OW distances are 3.3 Å). This is the only conformer in which the Cs^+ is not located within the plane formed by the water oxygens. The III conformer has the three water molecules simultaneously located in the first solvation shell of the cation (all three Cs^+-OW distances are 3.2 Å), and without hydrogen bonds. In conformer IV, the three water molecules are located within the first solvation shell of the cation, with Cs^+-OW distances of 3.1, 3.2 and 3.6 Å, at the B3LYP-D3 level. The difference with the III-conformer is that two waters are now forming a dimer. The B3LYP-D3 IV structure differs slightly from that obtained at the MP2 level[7, 8, 12] (and this work). At the MP2 level of representation, the water dimer is formed with a water molecule effectively located in the second shell of Cs^+ (5.4 Å for the Cs^+-OW distance at the MP2 level vs. 3.6 Å at the B3LYP-D3 level). This is the main structural difference between the B3LYP-D3 and MP2 optimized geometries over the I-IV structures.

As expected with weakly tagged clusters, several quasi-isoenergetic tagged-conformations are found within 9.0 kJ/mol. The I to IV energy ranking obtained for the untagged $Cs^+(H_2O)_3$ cluster is not affected by the presence of the tagged atom (Ar)/molecule (D_2), while the I-IV $Cs^+(H_2O)_3$ geometries are generally not modified by the presence of the tag. The only exception is the D_2-$Cs^+(H_2O)_3$ IV-6 conformer: the interaction with D_2 stabilizes a configuration in which one water molecule of the dimer is now located in the cation second solvation shell. Conformer IV-5 can be optimized only with Ar, while IV-6 can only be optimized with D_2. The 'OP' sign in Figure 2 (main text) refers to the location of the Ar/D_2 tag being located out-of-the plane formed by the oxygens of the water molecules.

To further test the reliability of the B3LYP-D3 electronic representation in describing the Ar/D_2–$Cs^+(H_2O)_3$ weak interactions, the DFT optimized geometries have been re-optimized at the MP2 level. Structures labeled I-4, I-5, I-6, II-4, IV-4, IV-5, and IV-6 of the Ar/D_2 tagged clusters cannot be found with the MP2 electronic representation. In these geometries, the Ar or D_2 tag is directly interacting with the Cs^+ cation. The MP2 electronic representation does not permit such close distance interactions to be energetically stable. All other geometries are stable with the MP2 electronic representation, and for these energetically stable conformers, the tag atom/molecule binding energy (BE) to the $Cs^+(H_2O)_3$ cluster not only agrees well in between the B3LYP-D3 and the MP2 levels but also with the experimental value of 4.2 kJ/mol.[12] Hence, the average BE obtained over the Ar-tagged I-conformers is 3.3 kJ/mol at the MP2 level and 4.2 kJ/mol at the B3LYP-D3 level, and 2.9/3.8 kJ/mol respectively for MP2 and B3LYP-D3 for the D_2-tagged clusters.

By tagging the I-conformer of $Cs^+(H_2O)_3$ one can see six isoenergetic stable structures (roughly within 1.0 kJ/mol), three structures have the Ar/D_2 tag weakly interacting with one water (I-1, I-2) or 3 waters (I-3), the other three structures having Ar/D_2 that interacts with the Cs cation. There are also six isoenergetic stable structures for the IV-conformer of $Cs^+(H_2O)_3$ (roughly within 1.0 kJ/mol of each others, and 7-8 kJ/mol higher in energy than the tagged I-conformer structures). Once again, three of them have the Ar/D_2 that interacts with one water and three of them have the tag that interacts with the Cs cation. There is no such structural diversity for the tagged II- and III-conformers, for which only two conformers are found.

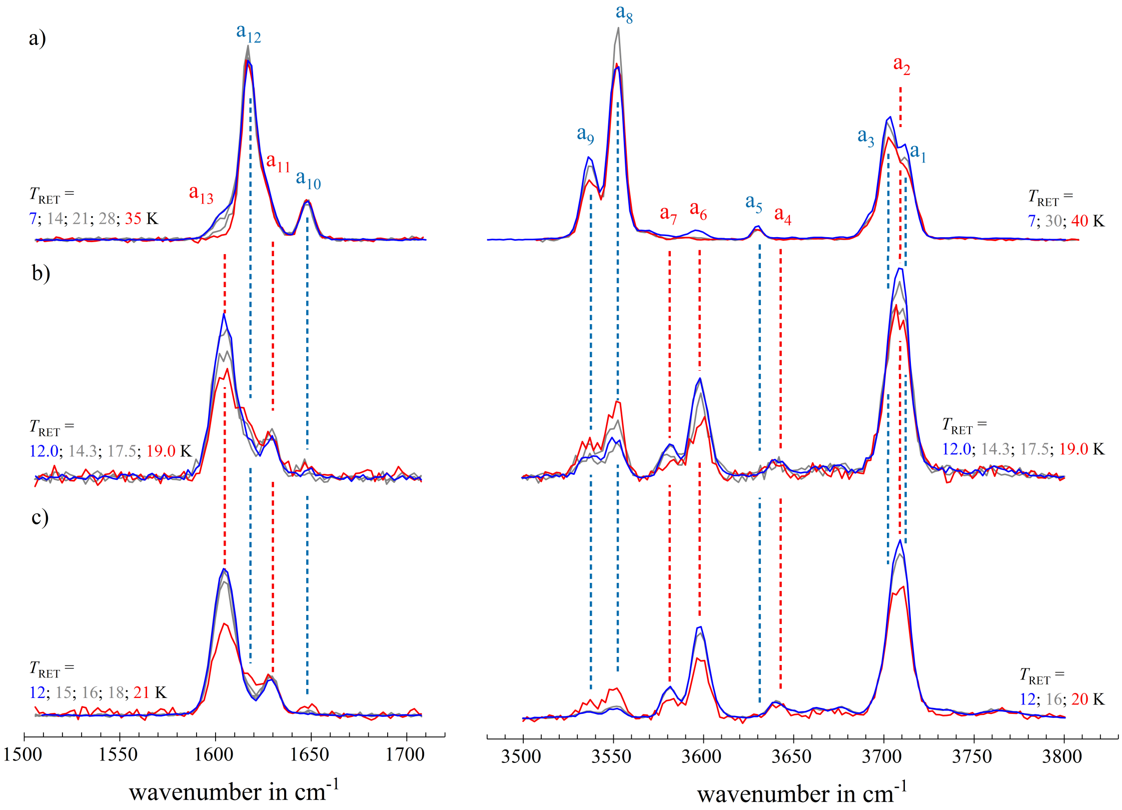

Figure S1. Temperature dependence of the IRPD spectra of a) $Cs^+(H_2O)_3\cdot Ar$, b) $Cs^+(H_2O)_3\cdot D_2$ where $Cs^+(H_2O)_3\cdot Ar$ was mass selected in the quadrupole mass filter and Ar was replaced by D_2 in the ion trap, and c) $Cs^+(H_2O)_3\cdot D_2$ where $Cs^+(H_2O)_3$ was mass selected and the complex was formed in the ion trap. Nominal ion trap temperatures are indicated in the figure.

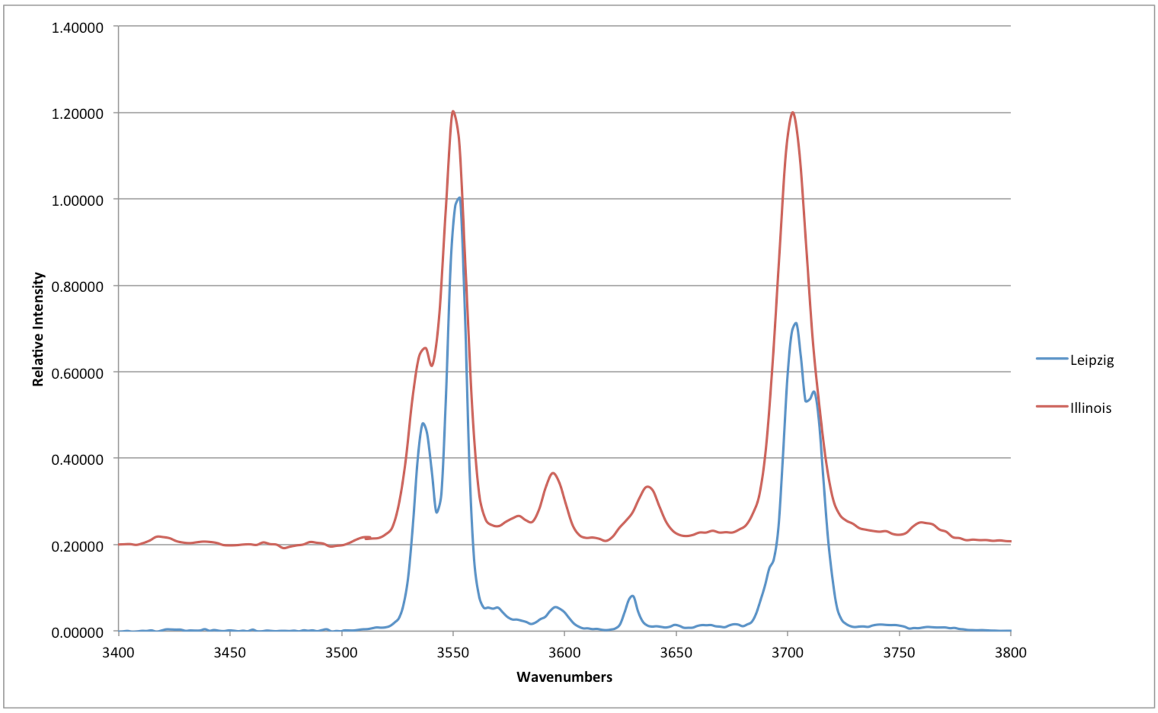

Figure S2. Spectra of $Cs^+(H_2O)_3Ar$ recorded at Illinois[12] and at Leipzig both formed by evaporative loss of argon, with the latter additionally cooled to 7 K by collisions with He in a ring electrode trap.

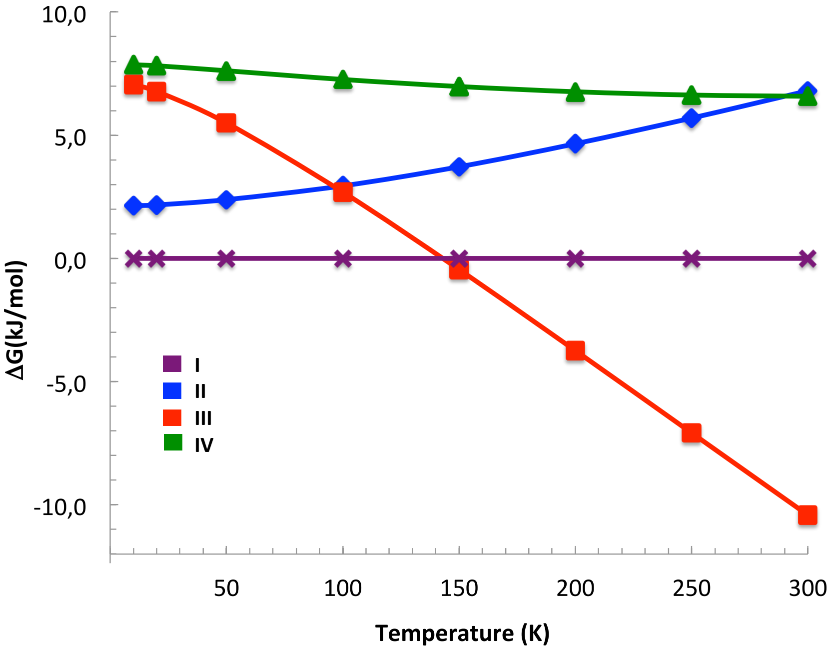

Figure S3. Free energy profiles as a function of increasing temperature calculated with the harmonic approximation. The relative free energy stability of the four untagged $Cs^+(H_2O)_3$ clusters (labeled I-IV) is hence shown. Comparison of this figure with Figure 6 in the main text, where free energy profiles have been calculated with DFT-MD biased metadynamics provides hints on anharmonic entropic effects.

Structural considerations

In both spectral regions, there is strong evidence for two different hydrogen-bond networks, one of which is stronger and more stable. In the OH stretching region, the stronger network has **lower** vibrational frequencies, with a larger shift from the gas-phase vibrational frequencies of isolated water (3657 and 3756 cm^{-1} for the symmetric and asymmetric OH stretches, respectively). In the H_2O bending region, the more stable and stronger network gives rise to bending frequencies that are shifted to **higher** vibrational frequencies, with a larger shift from the gas-phase bending frequency of 1595 cm^{-1}.

This is consistent with molecular structure calculations showing the more stable and stronger network, conformer I, with two water molecules in the first solvent shell directly bound to the cesium ion, with the third water molecule secured by two hydrogen bonds, one from each of the first shell waters. The weaker and less stable network, conformer IV, has three water molecules in the first shell with a weakened single hydrogen bond between two of the waters.

From these observations, it is clear that there are two different structural conformers that are preferentially formed with argon and D_2 messengers. When $Cs^+(H_2O)_3Ar$ is trapped directly at 7 K, the dominant configuration reflects stronger hydrogen bonding. This is supported by both the lower vibrational frequencies for the hydrogen-bonded OH stretches at 3538 and 3552 cm^{-1}, and the higher frequency H_2O bending frequencies at 1617 and 1648 cm^{-1} (the unperturbed H_2O bending frequency is at 1597 cm^{-1}). There is evidence for a second minor conformer when the trap temperature is less than ~30 K, with a band at 3598 cm^{-1} in the OH stretching region, and shoulders on either side of the 1617 cm^{-1}. The situation is reversed when $Cs^+(H_2O)_3Ar$ or $Cs^+(H_2O)_3$ are initially trapped and D_2 either replaces the argon or is directly attached to the hydrated ion. A second structural conformer, with hydrogen-bonded OH stretches at 3581 and 3598 cm^{-1}, and H_2O bending frequencies at 1604 and 1630 cm^{-1}, is now dominant when the trap temperature is 12 K. This second conformer has weaker hydrogen bonds as typified by a shift of ~+45 cm^{-1} for the hydrogen-bonded OH stretches, and ~-15 cm^{-1} for the H_2O bending frequencies.

References

1. G. W. T. M. J. Frisch, H. B. Schlegel, G. E. Scuseria, M. A. Robb, J. R. Cheeseman, G. Scalmani, V. Barone, G. A. Petersson, H. Nakatsuji, X. Li, M. Caricato, A. V. Marenich, J. Bloino, B. G. Janesko, R. Gomperts, B. Mennucci, H. P. Hratchian, J. V. Ortiz, A. F. Izmaylov, J. L. Sonnenberg, D. Williams-Young, F. Ding, F. Lipparini, F. Egidi, J. Goings, B. Peng, A. Petrone, T. Henderson, D. Ranasinghe, V. G. Zakrzewski, J. Gao, N. Rega, G. Zheng, W. Liang, M. Hada, M. Ehara, K. Toyota, R. Fukuda, J. Hasegawa, M. Ishida, T. Nakajima, Y. Honda, O. Kitao, H. Nakai, T. Vreven, K. Throssell, J. A. Montgomery, Jr., J. E. Peralta, F. Ogliaro, M. J. Bearpark, J. J. Heyd, E. N. Brothers, K. N. Kudin, V. N. Staroverov, T. A. Keith, R. Kobayashi, J. Normand, K. Raghavachari, A. P. Rendell, J. C. Burant, S. S. Iyengar, J. Tomasi, M. Cossi, J. M. Millam, M. Klene, C. Adamo, R. Cammi, J. W. Ochterski, R. L. Martin, K. Morokuma, O. Farkas, J. B. Foresman, and D. J. Fox, *Journal*, 2016.
2. S. Grimme, J. Antony, S. Ehrlich and H. Krieg, *Journal of Chemical Physics*, 2010, **132**.
3. S. Grimme, S. Ehrlich and L. Goerigk, *Journal of Computational Chemistry*, 2011, **32**, 1456-1465.
4. T. H. Dunning Jr., and Hay, J.P, in *Modern Theoretical Chemistry*, ed. H. F. S. III, Plenum, New York, 1977, vol. 3, pp. 1-28.
5. R. A. Kendall, T. H. Dunning Jr and R. J. Harrison, *The Journal of Chemical Physics*, 1992, **96**, 6796-6806.
6. J. P. Merrick, D. Moran and L. Radom, *Journal of Physical Chemistry A*, 2007, **111**, 11683-11700.
7. D. J. Miller and J. M. Lisy, *Journal of the American Chemical Society*, 2008, **130**, 15381-15392.
8. M. Kołaski, H. M. Lee, Y. C. Choi, K. S. Kim, P. Tarakeshwar, D. J. Miller and J. M. Lisy, *Journal of Chemical Physics*, 2007, **126**.
9. J. Hutter, M. Iannuzzi, F. Schiffmann and J. Vandevondele, *Wiley Interdisciplinary Reviews: Computational Molecular Science*, 2014, **4**, 15-25.
10. S. Goedecker and M. Teter, *Physical Review B - Condensed Matter and Materials Physics*, 1996, **54**, 1703-1710.
11. G. J. Martyna and M. E. Tuckerman, *Journal of Chemical Physics*, 1999, **110**, 2810-2821.
12. H. Ke, C. Van Der Linde and J. M. Lisy, *Journal of Physical Chemistry A*, 2015, **119**, 2037-2051.